varied by using different thermal models[22]. The depths of the earthquakes depend on the assumed crustal thickness and velocities in the upper lithosphere, but reasonable variation[23] would make a difference of no more than 1 km. A temperature of 600 °C is approximate but is consistent with the onset of ductile deformation in olivine-rich materials at probable strain rates[7]. The systematic difference between the two transforms is independent of these uncertainties. The depths of the earthquakes on the Romanche transform are deeper than previously determined for oceanic transform earthquakes; they are also in older lithosphere.

The degree of seismic coupling of oceanic transform faults has remained poorly constrained since it was first studied[24], because the width of the seismic zone was unknown. Our large seismic widths result in relatively low seismic slip rates (Fig. 5), only about half of the 37 mm yr^{-1} tectonic slip rate[25].

If we are not underestimating the seismic slip, then half of the slip must be occurring aseismically. It has been suggested that aseismic and slow (possibly precursory) slip might occur in the upper mantle, whereas higher speed seismic slip occurs in a very shallow seismogenic zone[4]. The depth extent of the seismic slip in the 1994 and 1995 earthquakes (Figs 3 and 5) and the centroid depths of the other events provide clear evidence of seismic rupture extending well into the upper mantle. Our results imply that significant aseismic slip is occurring and it is likely to be at shallow depths, perhaps within the serpentinized zone.

The depth of seismic slip on oceanic transform faults is controlled by temperature and is limited by the ~600 °C isotherm. The focal mechanisms of earthquakes of the two transform faults show impressive consistency, indicating that the faults are highly planar. We also find that the two previously identified[4] unusual aspects of the 1994 Romanche earthquake are probably artefacts of the analysis procedure used. No detectable precursors to oceanic transform earthquakes can be resolved unambiguously with present seismic data and analysis techniques. □

Received 1 March; accepted 11 December 2000.

1. Kanamori, H. & Stewart, G. S. Mode of the strain release along the Gibbs fracture zone, Mid-Atlantic Ridge. *Phys. Earth Planet. Inter.* **11,** 312–332 (1976).
2. Okal, E. A. & Stewart, L. M. Slow earthquakes along oceanic fracture zones: evidence for aesthenospheric flow away from hotspots? *Earth Planet. Sci. Lett.* **57,** 75–87 (1992).
3. Ihmlé, P. F. & Jordan, T. M. Teleseismic search for slow precursors to large earthquakes. *Science* **266,** 1547–1551 (1994).
4. McGuire, J. J., Ihmlé, P. F. & Jordan, T. H. Time domain observations of a slow precursor to the 1994 Romanche transform earthquake. *Science* **274,** 82–85 (1996).
5. Ihmlé, P. F., Harabaglia, P. & Jordan, T. H. Teleseismic detection of a slow precursor to the great 1989 Macquarie Ridge earthquake. *Science* **261,** 177–183 (1993).
6. Sibson, R. H. Fault zone models, heat flow and the depth distribution of earthquakes in the continental crust of the United States. *Bull. Seismol. Soc. Am.* **72,** 151–163 (1982).
7. Wiens, D. A. & Stein, S. Age dependence of oceanic intraplate seismicity and implications for lithospheric evolution. *J. Geophys. Res.* **88,** 6455–6468 (1983).
8. Engeln, J. F., Wiens, D. A. & Stein, S. Mechanisms and depths of Atlantic transform faults. *J. Geophys. Res.* **91,** 548–577 (1986).
9. Bergman, E. A. & Solomon, S. C. Transform fault earthquakes in the North Atlantic: source mechanisms and depth of faulting. *J. Geophys. Res.* **93,** 9027–9057 (1988).
10. Wilcock, W. S. D., Purdy, G. M. & Solomon, S. C. Microearthquake evidence for extensions across the Kane transform fault. *J. Geophys. Res.* **95,** 15439–15462 (1990).
11. Kanamori, H. & Kikuchi, M. The 1992 Nicaragua earthquake: a slow tsunami earthquake associated with subducted sediments. *Nature* **361,** 714–716 (1993).
12. Kedar, S., Watada, S. & Tanimoto, T. The 1989 Macquarie Ridge earthquake: seismic moment estimation from long period free oscillations. *J. Geophys. Res.* **99,** 17893–17907 (1994).
13. Velasco, A. A., Ammon, C. J. & Lay, T. Source time function complexity of the great 1989 Macquarie Ridge earthquake. *J. Geophys. Res.* **100,** 3989–4009 (1995).
14. Silver, P. G. & Jordan, T. H. Total-moment spectra of fourteen large earthquakes. *J. Geophys. Res.* **88,** 3273–3293 (1983).
15. Dziewonski, A. M. & Woodhouse, J. H. An experiment in systematic study of global seismicity: centroid-moment tensor solutions for 201 moderate and large earthquakes of 1981. *J. Geophys. Res.* **88,** 3247–3271 (1983).
16. Dziewonski, A. M., Ekström, G. & Maternovskaya, N.-N. Centroid-moment tensor solutions for October–December. *Phys. Earth Planet. Inter.* **115,** 1–16 (1999).
17. Abercrombie, R. E. & Mori, J. J. Local observations of the onset of a large earthquakes: 28 June 1992 Landers, California. *Bull. Seismol. Soc. Am.* **84,** 725–734 (1994).
18. Wesnousky, S. G. Seismological and structural evolution of strike-slip faults. *Nature* **335,** 340–343 (1988).
19. Harris, R. A. & Day, S. M. Dynamic 3D simulations of earthquakes on en echelon faults. *Geophys. Res. Lett.* **26,** 2089–2092 (1999).
20. Dziewonski, A. M. & Anderson, D. L. Preliminary reference Earth model. *Phys. Earth Planet. Inter.* **2,** 297–356 (1981).
21. Kanamori, H. & Anderson, D. L. Theoretical basis for some empirical relations in seismology. *Bull. Seismol. Soc. Am.* **65,** 1073–1095 (1975).
22. Chen, Y. Thermal model of oceanic transform faults. *J. Geophys. Res.* **93,** 8839–8851 (1988).
23. Detrick, R. S., White, R. S. & Purdy, G. M. Crustal structure of North Atlantic fracture zones. *Rev. Geophys.* **31,** 439–458 (1993).
24. Brune, J. N. Seismic moment, seismicity and rate of slip along major fault zones. *J. Geophys. Res.* **73,** 777–784 (1968).
25. DeMets, C., Gordon, R. G., Argus, D. F. & Stein, S. Current plate motions. *Geophys. J. Int.* **101,** 425–478 (1990).
26. Smith, W. H. F. & Sandwell, D. T. Global sea floor topography from satellite altimetry and ship depth soundings. *Science* **277,** 1956–1962 (1997).
27. Wessel, P. & Smith, W. H. F. Free software helps map and display data. *Eos* **72,** 441, 445–446 (1991).
28. Ekström, G. A very broadband inversion method for the recovery of earthquake source parameters. *Tectonophysics* **166,** 73–100 (1989).
29. Antolik, M., Kaverina, A. & Dreger, D. Compound rupture of the great 1998 Antarctic plate earthquake. *J. Geophys. Res.* **105,** 23825–23838 (2000).
30. McKenzie, D. P. Speculations on the consequences and causes of plate motions. *Geophys. J. R. Astron. Soc.* **18,** 1–32 (1969).

Acknowledgements

We thank M. Antolik for assistance with the slip inversion, and J. Tromp for discussion.

Correspondence and requests for materials should be addressed to R. E. A. (e-mail: rachel@seismology.harvard.edu).

Isotopic evidence for microbial sulphate reduction in the early Archaean era

Yanan Shen*, Roger Buick† & Donald E. Canfield*

** Danish Center for Earth System Science (DCESS) and Institute of Biology, Odense University, SDU, Campusvej 55, 5230 Odense M, Denmark*
† School of Geosciences FO5, University of Sydney, Sydney, NSW 2006, Australia

Sulphate-reducing microbes affect the modern sulphur cycle, and may be quite ancient[1,2], though when they evolved is uncertain. These organisms produce sulphide while oxidizing organic matter or hydrogen with sulphate[3]. At sulphate concentrations greater than 1 mM, the sulphides are isotopically fractionated (depleted in ^{34}S) by 10–40‰ compared to the sulphate, with fractionations decreasing to near 0‰ at lower concentrations[2,4–6]. The isotope record of sedimentary sulphides shows large fractionations relative to seawater sulphate by 2.7 Gyr ago, indicating microbial sulphate reduction[7]. In older rocks, however, much smaller fractionations are of equivocal origin, possibly biogenic but also possibly volcanogenic[2,8–10]. Here we report microscopic sulphides in ~3.47-Gyr-old barites from North Pole, Australia, with maximum fractionations of 21.1‰, about a mean of 11.6‰, clearly indicating microbial sulphate reduction. Our results extend the geological record of microbial sulphate reduction back more than 750 million years, and represent direct evidence of an early specific metabolic pathway—allowing time calibration of a deep node on the tree of life.

Our samples came from the Dresser Formation (Warrawoona Group, Pilbara Craton) at North Pole in northwestern Australia. These rocks have experienced only very-low-grade metamorphism and slight deformation[11]. Their age is constrained by zircon U–Pb geochronology to 3.515–3.458 Gyr (ref. 12). The Dresser Formation consists of pillowed, amygdaloidal basalt with three interbeds of cherty metasediments. Most samples came from the lowest chert bed, from lenses of bedded barite ($BaSO_4$) within silicified volcanogenic and carbonate sediments that were deposited in a shallow subaqueous to intermittently exposed setting[13]. Other samples are from barite veins transecting and underlying the chert units. The barite beds are sedimentary deposits, indicated by crystals that were draped by detrital sediment (Fig. 1a), or were eroded and rounded during clastic redeposition. Measurements of interfacial angles show that the barite crystals were originally composed of gypsum ($CaSO_4 \cdot 2H_2O$)[11,14], which precipitated in evaporating brine ponds separated from the sea by a permeable pumiceous sand bar[15]. Low sulphate concentrations in sea water seeping into the brine ponds may have been locally supplemented by the phototrophic oxidation of volcanogenic sulphide[11].

In much of the original gypsum, isomorphous substitution of Ba^{2+} for Ca^{2+} ('baritization') occurred soon after burial when relatively cool hydrothermal fluids circulated through the surrounding basalt pile[11]. About 30% excess sulphate is required for isomorphous replacement because of differences in unit cell volume between parent gypsum and daughter barite. This extra sulphate was probably derived locally from the bedded gypsum where some of the original gypsum is now replaced by quartz[11], from dispersed sedimentary gypsum now also replaced by quartz[11], and from pore fluids. The hydrothermal fluids were an unlikely source of sulphate because the very low solubility of barite requires that Ba^{2+} and SO_4^{2-} cannot be transported together in solution. Sulphate remobilized from sedimentary gypsum could also have contributed to barite precipitation in the crosscutting veins. Thus, the barite veins may represent conduits for hydrothermal fluid circulation[16], where upwelling Ba^{2+} solutions mixed with surficial sulphate-containing solutions.

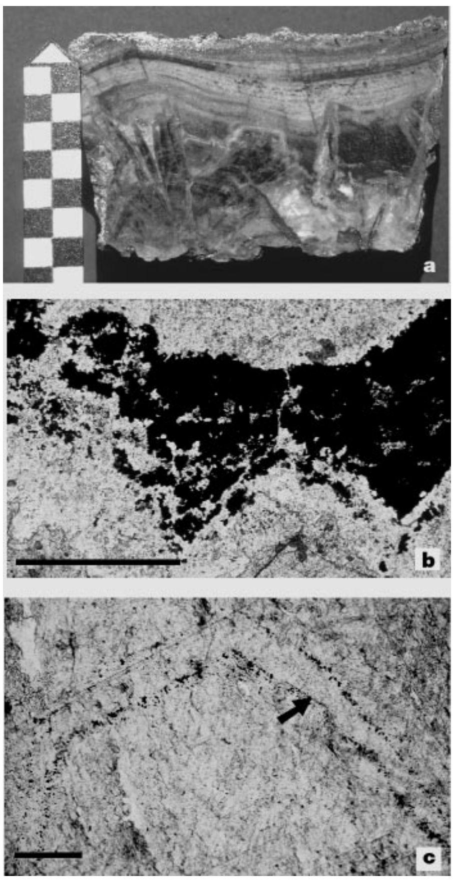

Figure 1 Relationships between sulphur species at North Pole, Australia. **a**, Laminae of silicified volcaniclastic/carbonate sediment draping over dark grey crystals of bedded barite, indicating a sedimentary origin for the precursor evaporative gypsum. The scale has 1-cm blocks, with an arrow pointing towards stratigraphic top. **b**, Opaque pyrite lamination (black) between barite beds draping over individual barite crystals. Scale bar, 1 mm. **c**, Microscopic sulphides (black, arrowed) included within a bedded crystal and aligned along growth faces of the precursor gypsum crystal. Scale bar, 1 mm.

Between the barite beds are undulating laminae 2–10 mm thick composed of macroscopic pyrite (Fig. 1b), now usually weathered to iron oxides but preserved in subsurface samples. Within the barite are microscopic sulphide crystals ~50 μm in size comprising less than 1% of the rock. These sulphides, mostly pyrite but some sphalerite, are aligned along growth faces of the original gypsum crystals (Fig. 1c). This attests to the syngenesis of sulphate and microscopic sulphide, and confirms that most sulphate is residual from the precursor gypsum. Also within the barite crystals are H_2S-containing fluid inclusions ~10 μm in size, apparently formed during crystal growth[17]. Barite in the transecting veins contains fine, disseminated pyrite crystals, but lacks pyrite laminae and sulphureous fluid inclusions. Organic matter is finely dispersed throughout the bedded barite, but is absent from the vein barite.

Previous isotopic analyses of the macroscopic pyrite laminae revealed an average isotopic composition ($\delta^{34}S$; see Fig. 2 legend) of –0.9‰ (s.d. = 1.5)[14], somewhat ^{34}S-depleted compared with the mantle value of 0‰. Our data (Fig. 2; full analytical data available as Supplementary Information) are similar, though slightly more depleted in ^{34}S (–2.4‰ ± 0.8). While these pyrites could represent unfractionated volcanogenic sulphur, they are consistently more ^{34}S-depleted than is typical of younger volcanogenic sulphide deposits[18]. However, they are not sufficiently ^{34}S-depleted to be definitely biological, so their origin is still equivocal[11].

By contrast, the previously unanalysed microscopic sulphides are highly ^{34}S-depleted (Fig. 2), with fractionations relative to coexisting sulphate ($\epsilon_{sulphide}$) ranging from 21.1‰ to 7.4‰, with a mean of 11.6‰. Fractionations in the same range (21.3–5.8‰) are also produced if we calculate relative to the average isotopic composition of sulphate in the bedded barite. Non-biological processes can, in principle, produce $\epsilon_{sulphide}$ values of this magnitude. For example, hydrolysis of SO_2 to sulphate and sulphide occurs in relatively oxidizing magmatic fluids as temperatures drop below 400 °C, forming H_2S depleted in ^{34}S by 15–20‰ relative to sulphate[18]. However, the rocks surrounding the North Pole deposits are mafic[11] and would have generated reduced rather than oxidized magmatic fluids. Furthermore, ^{34}S-depleted sulphides precipitated with sulphates from Archaean magmatic fluids are usually associated with pervasive haematite deposition[19], absent from the North Pole barite deposits. Therefore, the hydrolysis of SO_2 is an unlikely explanation for our results.

Alternatively, inorganic reduction of sulphate to sulphide by ferrous minerals can occur at near-neutral pH and temperatures greater than 200 °C (ref. 18), with equilibrium $\epsilon_{sulphide}$ ranging from 27‰ at 200 °C to ~10‰ at 550 °C (ref. 18). A recirculating hydrothermal system with sulphate entrained from the brine ponds could conceivably have produced ^{34}S-depleted sulphides during partial sulphate reduction in hot underlying basalts. A spectrum of isotope values could, in principle, result from variable sulphate depletion or fluctuating temperatures during hydrothermal sulphate reduction. Our results, however, are largely outside the range, –5‰ to +9‰, generally found for high-temperature hydrothermal sulphate reduction[8].

Furthermore, the original sulphate mineral was gypsum, not anhydrite or barite, the two typical hydrothermal sulphates. Gypsum is only stable below ~60 °C (ref. 20), so the alignment of the microscopic sulphides along the crystal faces of the original gypsum (Fig. 1c) indicates that these sulphides were formed at relatively low temperatures along with the original gypsum. These microscopic sulphides were, therefore, formed before baritization, the earliest known hydrothermal event at North Pole[13]. We thus find no compelling evidence for a magmatic or hydrothermal origin for the microscopic sulphides in the bedded barites at North Pole. Given the early formation of the microscopic sulphides at low temperature, a metamorphic origin is also unlikely.

The fractionations between sulphate and microcrystalline sulphides at North Pole are within the range observed for modern sulphate-reducing microbes metabolizing with > 1 mM sulphate, especially for organisms growing at high specific rates of sulphate reduction where ϵ_{SR} (fractionation during sulphate reduction) values of 10‰ to 25‰ are typical[5]. Moreover, the sulphides are intimately associated with organic carbon, the principal electron donor for biological sulphate reduction. These features, together with the lack of evidence for non-biological sources of highly fractionated sulphide, demonstrate that microbial sulphate reduction had evolved by 3.47 Gyr ago. Sulphate reduction is evident here because the North Pole evaporite ponds were localized oases of high sulphate concentrations, containing organic electron donors produced by an indigenous stromatolitic microbiota[15], providing favourable conditions for sulphate-reducers to generate high fractionations. This contrasts with open marine Archaean settings, where only small fractionations of ~0‰ were expressed due to low sulphate concentrations and hence low atmospheric oxygen levels[21].

Sulphides from the vein barites have a similar spread in $\epsilon_{sulphide}$ values as the bedded barites, ranging from 16.1‰ to 3.4‰. While the veins may have fed hydrothermal fluids to the sedimentary barite beds[16], the vein sulphides show no evidence for a magmatic, hydrothermal or metamorphic origin. It is more likely that these sulphides were biogenic, although it is unclear whether they were formed *in situ* or remobilized from surficial environments. However, the absence of sulphureous fluid inclusions in the vein barite suggests the latter.

Our results provide the oldest evidence of microbial sulphate reduction in the geological record, pre-dating previous evidence[7] by more than 0.75 Gyr (Fig. 3). They also give the earliest indication of a specific microbial metabolism. Though the isotopic record of organic carbon suggests that autotrophic CO_2 fixation into biomass had evolved by ~3.8 Gyr ago[22,23], the specific metabolic pathways employed, and the organisms responsible, are unclear. Likewise, although microfossil evidence is permissive of cyanobacteria by 3.45 Gyr ago[24], these simple forms are not diagnostic of a specific microbial affinity or a particular metabolic pathway[6]. Sulphate reduction is a complex metabolic process requiring advanced membrane-bound transport enzymes, proton motive force generation by ATPase and other charge separation proteins, and the genetic regulation of protein synthesis through DNA and RNA[25]. Therefore, by 3.47 Gyr ago—and probably earlier as the known pathways of CO_2 fixation are also complex—microbes had already developed many of the critical cellular systems shared by their modern descendants.

Dissimilatory sulphate reduction occurs in both the Archaeal and Bacterial domains of the tree of life as deduced from small-subunit ribosomal RNA (SSU rRNA). Among the Archaea, the only known

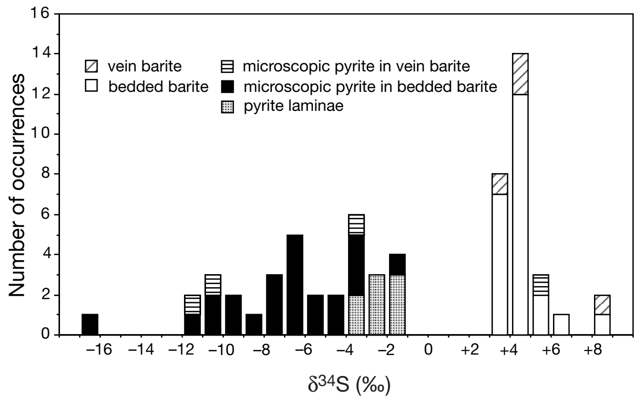

Figure 2 The isotopic composition of sulphur species from the barite deposits of North Pole, Australia. $\delta^{34}S = 1{,}000\{[(^{34}S/^{32}S)_{sample}/(^{34}S/^{32}S)_{standard}]\} - 1$ relative to the Cañon Diablo Troilite standard.

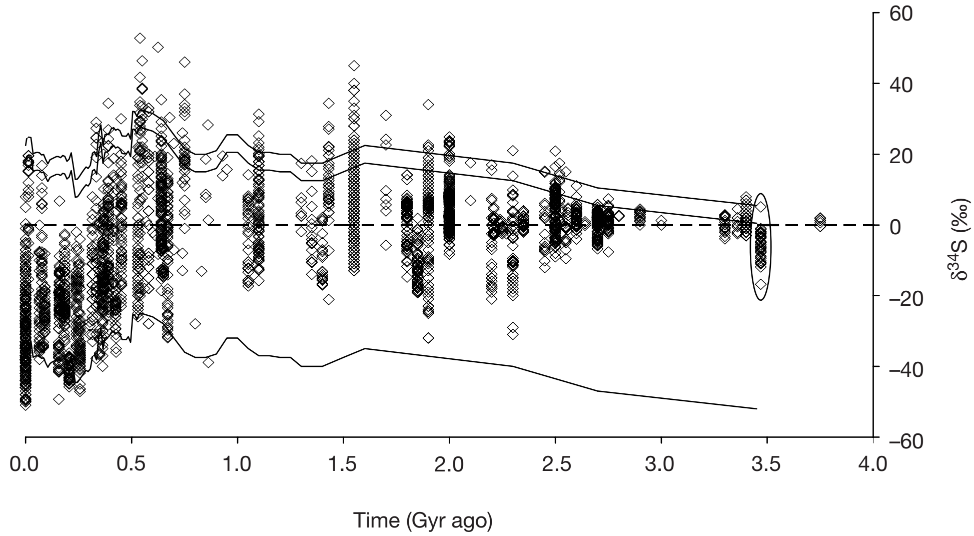

Figure 3 The secular trends in the isotopic composition of seawater sulphate and sulphide over geological time. Data within the oval are from this work, the other data are from refs 2, 29. The band (double line) in the upper part of the figure represents the isotopic composition of seawater sulphate through time. The single line in the lower part of the figure is displaced from the seawater sulphate trend by 55‰, representing the maximum fractionation between sulphate and sulphide through the past 600 million years. Before 1.7 Gyr ago, constraints on the isotopic composition of seawater sulphate are sparse.

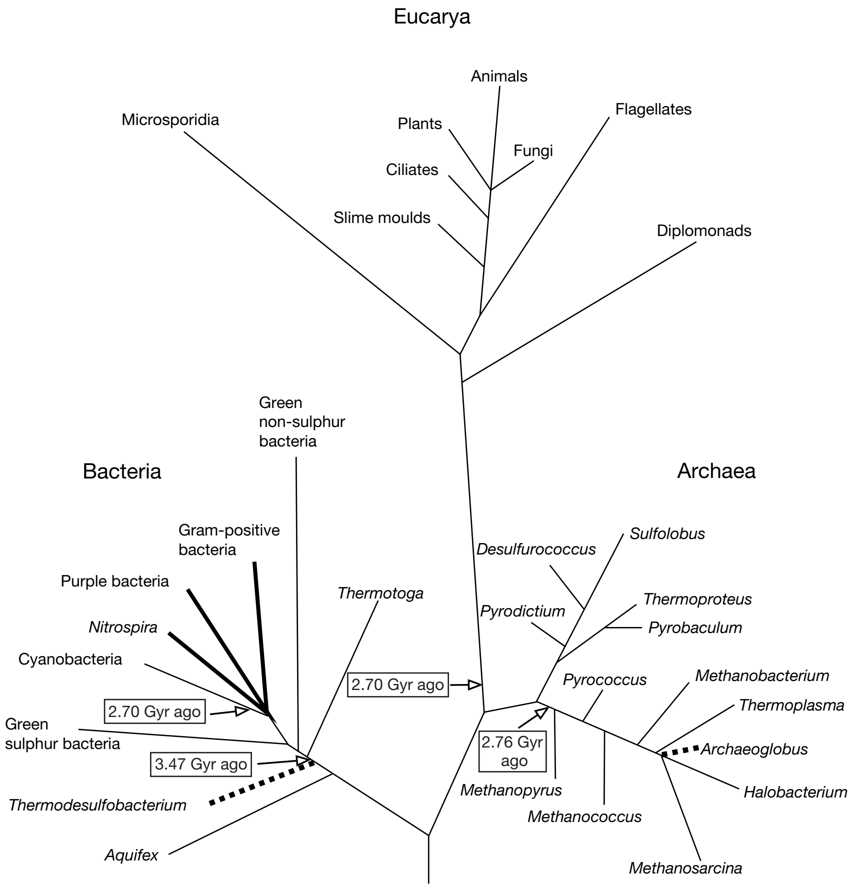

Figure 4 The tree of life based on SSU rRNA sequence analysis, with some temporal constraints on branching. The tree is modified from ref. 2, and abstracted from phylogenetic trees presented in refs 26 and 27. The time calibration points are from ref. 30, with our additional constraint of 3.47 Gyr placed in the Bacterial domain. Lineages housing sulphate-reducers metabolizing at temperatures > 70 °C are shown by broken black lines, while lineages supporting sulphate-reducers metabolizing at < 70 °C are shown by heavy black lines.

sulphate-reducers are hyperthermophiles with optimal growth temperature above 80 °C, and these are restricted to the single genus *Archaeoglobus*[26]. Within the Bacteria, the most deeply branching sulphate-reducers belong to the genus *Thermodesulfobacterium*[2,27], which are also hyperthermophiles with optimal growth around 80 °C. Thus far, sulphate reduction by organisms metabolizing at temperatures below 70 °C is known only from the δ-subdivision of the proteobacteria (purple bacteria), the Gram-positive bacteria, and the Nitrospira group (Fig. 4). As only a small proportion of total microbial diversity has been characterized[27], it is possible that the ability to reduce sulphate at moderate temperatures resides elsewhere in prokaryote phylogeny.

As the original gypsum now forming the bedded barites at North Pole first precipitated at temperatures below 60 °C, the organisms responsible for sulphate reduction were apparently mesophiles or, at most, moderate thermophiles. Given what is currently known about the phylogenetic distribution of temperature adaptations among sulphate-reducers, our findings suggests a minimum age of 3.47 Gyr for a node immediately above the branching point of the hyperthermophilic *Thermodesulfobacterium* lineage in the Bacterial domain (Fig. 4). This placement is necessarily tentative, as deeper-branching mesophilic sulphate-reducers may be discovered, but even so it represents the oldest evolutionary event thus far dated on the tree of life. □

Methods

Macroscopic pyrites were sampled with a dental drill, microscopic sulphides were distilled from the enclosing barite by Cr-reduction[28] and collected as Ag_2S, and residual barite was collected after Cr-reduction. Isotope analysis was performed in two ways. For large samples, SO_2 gas was generated from both pyrite and barite by heating the sulphur samples to 1,050 °C and 1,150 °C, respectively, with cuprous oxide. The SO_2 gas was purified on a high-vacuum gas extraction line and subsequent isotope analyses were reproducible to better than ±0.5‰. Small samples of barite and Ag_2S were combusted directly to SO_2 in an elemental analyser coupled directly to an isotope ratio mass spectrometer (isotope analyses reproducible to ±0.3‰). Comparison of both techniques on homogenized splits of the same samples showed an average difference of 0.24‰ ($n = 5$).

Received 18 May; accepted 24 November 2000.

1. Wagner, M., Roger, A. J., Flax, J. L., Brusseau, G. A. & Stahl, D. A. Phylogeny of dissimilatory sulfite reductases supports an early origin of sulfate respiration. *J. Bacteriol.* **180,** 2975–2982 (1998).
2. Canfield, D. E. & Raiswell, R. The evolution of the sulfur cycle. *Am. J. Sci.* **299,** 697–723 (1999).
3. Postgate, J. R. *The Sulphate-Reducing Bacteria* 2nd edn (Cambridge Univ. Press, Cambridge, 1984).
4. Harrison, A. G. & Thode, H. G. Mechanisms of the bacterial reduction of sulphate from isotope fractionation studies. *Trans. Faraday Soc.* **53,** 84–92 (1958).
5. Kaplan, I. R. & Rittenberg, S. C. Microbiological fractionation of sulphur isotopes. *J. Gen. Microbiol.* **34,** 195–212 (1964).
6. Knoll, A. H. & Canfield, D. E. Isotopic inferences on early ecosystems. *Paleontol. Soc. Pap.* **4,** 212–243 (1998).
7. Goodwin, A. M., Monster, J. & Thode, H. G. Carbon and sulfur isotope abundances in Archean iron-formations and early Precambrian life. *Econ. Geol.* **71,** 870–891 (1976).
8. Cameron, E. M. Sulphate and sulphate reduction in early Precambrian. *Nature* **296,** 145–148 (1982).
9. Hayes, J. M., Lambert, I. B. & Strauss, H. in *The Proterozoic Biosphere: A Multidisciplinary Study* (eds Schopf, J. W. & Klein, C.) 129–134 (Cambridge Univ. Press, Cambridge, 1992).
10. Ohmoto, H., Kakegawa, T. & Lowe, D. R. 3.4-billion-year-old biogenic pyrites from Barberton, South Africa: sulfur isotope evidence. *Science* **262,** 555–557 (1993).
11. Buick, R. & Dunlop, J. S. R. Evaporitic sediments of early Archaean age from the Warrawoona Group, North Pole, Western Australia. *Sedimentology* **37,** 247–277 (1990).
12. Buick, R. *et al.* Record of emergent continental crust ~3.5 billion years ago in the Pilbara Craton of Australia. *Nature* **375,** 574–577 (1995).
13. Buick, R. & Barnes, K. R. Cherts in the Warrawoona Group: early Archaean silicified sediments deposited in shallow water environments. *Univ. West. Aust. Geol. Dept Univ. Extension Spec. Publ.* **9,** 37–53 (1984).
14. Lambert, I. B., Donnelly, T. H., Dunlop, J. S. R. & Groves, D. I. Stable isotope compositions of early Archaean sulphate deposits of probable evaporite and volcanogenic origins. *Nature* **276,** 808–810 (1978).

15. Groves, D. I., Dunlop, J. S. R. & Buick, R. An early habitat of life. *Sci. Am.* **245,** 64–73 (1981).
16. Nijman, W., de Bruijne, K. C. H. & Valkering, M. E. Growth fault control of Early Archaean cherts, barite mounds and chert-barite veins, North Pole Dome, Eastern Pilbara, Western Australia. *Precambr. Res.* **88,** 25–52 (1999).
17. Rankin, A. H. & Shepherd, T. J. H_2S-bearing fluid inclusions in baryte from the North Pole deposit, Western Australia. *Mineral. Mag.* **42,** 408–410 (1978).
18. Ohmoto, H. & Goldhaber, M. B. in *Geochemistry of Hydrothermal Ore Deposits* (ed. Barnes, H. L.) 517–611 (Wiley, New York, 1997).
19. Cameron, E. M. & Hattori, K. Archean gold mineralization and oxidized hydrothermal fluids. *Econ. Geol.* **82,** 1177–1191 (1987).
20. Hardie, L. A. The gypsum-anhydrite equilibrium at one atmosphere pressure. *Am. Mineral.* **52,** 171–200 (1967).
21. Canfield, D. E., Habicht, K. S. & Thamdrup, B. The Archean sulfur cycle and the early history of atmospheric oxygen. *Science* **288,** 658–661 (2000).
22. Schidlowski, M. A 3800-million-year isotopic record of life from carbon in sedimentary rocks. *Nature* **333,** 313–318 (1988).
23. Rosing, M. T. ^{13}C-depleted carbon microparticles in >3700-Ma sea-floor sedimentary rocks from west Greenland. *Science* **283,** 674–676 (1999).
24. Schopf, J. W. & Packer, B. M. Early Archean (3.3-billion to 3.5-billion-year-old) microfossils from the Warrawoona Group, Australia. *Science* **237,** 70–73 (1987).
25. Widdel, F. in *Biology of Anaerobic Microorganisms* (ed. Zehnder, A. J. B.) 496–585 (Wiley, New York, 1988).
26. Stetter, K. O. in *Evolution of Hydrothermal Ecosystems on Earth (and Mars?)* (eds Bock, G. R. & Goode, J. A.) 1–10 (Wiley, New York, 1996).
27. Pace, N. R. A molecular view of microbial diversity and the biosphere. *Science* **276,** 734–740 (1997).
28. Canfield, D. E., Raiswell, R., Westrich, J. T., Reaves, C. M. & Berner, R. A. The use of chromium reduction in the analysis of reduced inorganic sulfur in sediments and shales. *Chem. Geol.* **54,** 149–155 (1986).
29. Canfield, D. E. A new model for Proterozoic ocean chemistry. *Nature* **396,** 450–453 (1998).
30. Knoll, A. H. A new molecular window on early life. *Science* **285,** 1025–1026 (1999).

Supplementary information is available on *Nature*'s World-Wide Web site (http://www.nature.com) or as paper copy from the London editorial office of *Nature*.

Acknowledgements

We thank J. S. R. Dunlop for suggesting that we should examine the isotopic systematics of microscopic sulphur species in the North Pole barite; K.-U. Hinrichs, K. Londry, R. Summons, B. Thamdrup and K. Habicht for discussions; I. O'Brien, O. Thomas and L. Salling for technical assistance; and D. Des Marais for comments and suggestions. This work was supported by the Danish Grundforkningsfond (Basic Research Foundation) and by the Australian Research Council (R.B.).

Correspondence and requests for materials should be addressed to Y.S. (e-mail: shen@biology.ou.dk).

A primitive sarcopterygian fish with an eyestalk

Min Zhu*, **Xiaobo Yu†** & **Per E. Ahlberg‡**

* *Institute of Vertebrate Paleontology and Paleoanthropology, Chinese Academy of Sciences, PO Box 643, Beijing 100044, China*
† *Department of Biological Sciences, Kean University, Union, New Jersey 07083, USA*
‡ *Department of Palaeontology, The Natural History Museum, Cromwell Road, London SW7 5BD, UK*

The discovery of two Early Devonian osteichthyan (bony fish) fossils[1–4] has challenged established ideas about the origin of osteichthyans and their divergence into actinopterygians (teleosts and their relatives) and sarcopterygians (tetrapods, coelacanths, lungfishes and related groups)[5–7]. *Psarolepis* from China[1,2,8,9] and an unnamed braincase from Australia[3] combine derived sarcopterygian and actinopterygian characters with primitive features previously restricted to non-osteichthyans, suggesting that early osteichthyan evolution may have involved substantial parallellism between sarcopterygians and actinopterygians. But interpretation of these fossils has been hampered by poor phylogenetic resolution[1,3]. Here we describe a basal sarcopterygian fish, *Achoania* gen, et sp. nov., that fills the morphological gap between *Psarolepis* and higher sarcoptergyians. We also report the presence of eyestalk attachments in both *Achoania* and *Psarolepis*, showing that this supposedly non-osteichthyan feature occurs in basal sarcopterygians as well as the actinoptergyian-like Australian braincase[3].

Sarcopterygii (Romer, 1955)
Achoania gen. nov.

Diagnosis. A sarcopterygian with an anteroventrally sloping intracranial joint; robust and rod-like premaxilla that lacks a posterodorsal process and does not contribute to the orbital margin; toothed median rostral that does not separate the premaxillae; large internasal cavities occupying about 33% of the length of the ethmosphenoid floor; small drop-shaped parasphenoid flanked by flat roughened surface; robust postorbital pila; large descending processes on ventral surface of sphenoidal region; very wide suborbital ledge; and prominent eyestalk scar. The external bones are covered by large-pore cosmine similar to that in *Psarolepis*.
Type species. *Achoania jarvikii* sp. nov.
Diagnosis. As for genus.
Etymology. Generic name referring to the absence of choana, from Greek *a* (not) and *choane* (funnel). Specific name in honour of the late Erik Jarvik.
Holotype. V6235, a fairly complete anterior cranial portion, IVPP, Beijing.
Locality and horizon. Qujing, E. Yunnan, China. Xitun Formation (late Lochkovian, Early Devonian)
Remarks. The new genus is represented by one anterior cranial portion (Fig. 1), which differs substantially from *Psarolepis* in the shape of the premaxilla, the parasphenoid, the internasal cavity (which occupies more than 70% of the length of the ethmosphenoid floor in *Psarolepis*), the postorbital pila and structures on the ventral side of the sphenoid. All the anterior cranial portions of *Psarolepis* are uniformly distinct from *Achoania* with no intermediate variations, and the posterior cranial specimens and lower jaws of *Psarolepis* fail to match the morphology of *Achoania*.
Description. The most impressive feature of *Achoania* gen. et sp. nov., is a heart-shaped unfinished area (Fig. 1c, d) in the interorbital wall, which lies immediately behind the optic canal and has outward-facing edges. Two small cup-shaped recesses lie posterodorsal and ventral to this area, the posterodorsal recess supported by a posteriorly running horizontal ridge. By comparison with placoderms[7,10], primitive chondrichthyans[7,11] and the Australian braincase (AMF101607)[3,4], the unfinished area represents the eyestalk attachment area, and the two small recesses represent sites for eye muscle attachment.

Except for its recently reported presence in AMF101607 (ref. 3), an eyestalk had been considered to exist only in two non-osteichthyan groups, chondrichthyans and the extinct placoderms. The presence of an eyestalk area in *Achoania* is corrobrated by the discovery of a similar structure in a newly collected *Psarolepis* specimen (Fig. 2), which shows, on both sides of the interorbital wall, a large unfinished area with well-defined margins between the optic nerve canal and pituitary vein canal. In addition, re-examination of a previously described specimen (V8136)[9] reveals a similarly positioned, although distorted, unfinished area on the exposed side of the interorbital wall. The well-preserved eyestalk area on both sides of the new *Psarolepis* specimen and the similar arrangement of foramina, pits and ridges in the interorbital wall of *Psarolepis* and *Achoania* strongly indicate that the eyestalk area in these two forms is a natural structure rather than an artefact of preservation or preparation. The eyestalk should now be considered a general gnathostome feature retained by early osteichthyans on both the actinopterygian and sarcopterygian lineages.

In other cranial features, *Achoania* resembles *Psarolepis* and differs from previously known sarcopterygians in having large, closely spaced pores on the cosmine surface, an anterodorsally facing anterior nostril, a toothed median rostral, a straight rather than lyre-shaped trajectory of the supraorbital sensory canal and a

